Engineering and Technology Journal
Journal homepage: https://etj.uotechnology.edu.iq

The effective of the passive and active techniques on the vibration control system

Firas A. Jasim, Mohammed J. Mohammed*, Hatam K. Kadhom

Electromechanical Engineering Dept., University of Technology-Iraq, Alsina'a street, 10066 Baghdad, Iraq.
*Corresponding author Email: mohammed.j.mohammed@uotechnology.edu.iq

HIGHLIGHTS

- An open-shaped wind tunnel was designed to provide wind speeds from 1 to 10 m/s for testing.
- A hollow aluminum cylinder, spring-mounted on circular plates, was designed to study vibration control.
- Passive control with double control rods (CRBCP) and active control using 12 V motors reduced vibrations.
- Optimal vibration reduction was achieved at 5 m/s wind speed with actuators at 84% motor speed and 12 V.

Keywords:

Wind-induced vibration

Open loop control strategy

Control rods Actuator

Vortex-Induced Vibration

Active Vibration Control

ABSTRACT

The interaction between structures and fluid flow in a direction perpendicular to the body can induce vibrations in the structure, a phenomenon known as vortex-induced vibration (VIV). This phenomenon may lead to structural failure due to resonance, which occurs when the natural frequency of the structure matches the vortex shedding frequency. Therefore, it is essential to employ vibration control devices to address the resulting high-amplitude instabilities. In this study, a subsonic wind tunnel with open-circuit specifications was constructed. This open-type wind tunnel generates airflow at varying velocities through the test section. To control vibrations around the cylindrical pipe, an Open-Loop Active Vibration Control (OLAVC) system is proposed. This system utilizes dual control rods, made of hollow stainless steel, driven by two DC motors positioned at the upper and lower sides of the main cylindrical pipe, referred to as the CRBCP (Control Rod-Based Cylinder Pipe). The effectiveness of a passive control strategy was evaluated prior to energizing the DC motors at 12 V. The results indicated that passive control alone was insufficient to adequately suppress the vibrations of the cylinder pipe. Subsequently, the OLAVC procedure was implemented using several voltage levels—12 V, 10 V, 8 V, and 6 V—corresponding to 100, 83, 75, and 50% of motor power, respectively. The OLAVC system proved effective in reducing vibrations across all actuator configurations. The maximum suppression, reaching 79.05%, was achieved at a motor voltage of 12 V and a rotational speed of 2349 rpm.

1. Introduction

Various structures, including suspension bridges, risers, cables, transmission pipes, nuclear fuel rods, heat exchangers, and even high-rise buildings, can potentially experience Wind wind-induced vibration (WIV) due to the flow [1]. In an attempt to reduce construction costs, modern structures have become lighter and less rigid and thus more susceptible to wind excitation. Vortex-induced vibration (VIV), in which the vortex-shedding frequency synchronizes with the natural frequency of the structure, transferring energy from the flow to the structure followed by high amplitude oscillations [2]. These oscillations are of tremendous importance, not only because of the enormous response amplitude, which may over-stress the structural part, but also because of the long-term cyclic stresses, which may induce fatigue failure [3]. The phenomena may occur with both bluff and streamlined forms, and it has been seen in various domains, including aeronautical engineering, mechanical engineering, civil engineering, and ocean engineering [4]. When a bluff body is subjected to fluid flow, a separated flow is generated over a portion of its surface. The flow around a bluff body is sensitive to Reynold's number (R_e). The dimensionless Reynolds number can be calculated with the following in Equation 1 [5].

$$R_e = \frac{\rho u D}{\mu} \quad (1)$$

http://doi.org/10.30684/etj.2025.155222.1849
Received 15 November 2024; Received in revised form 25 February 2025; Accepted 07 March 2025; Available online 05 May 2025
2412-0758/University of Technology-Iraq, Baghdad, Iraq

ρ is the fluid density, u is the free-stream velocity of the fluid, μ is the kinematic viscosity, and D is the outer diameter of the bluff body. The dimensionless parameter is the reduced velocity (U_r) in Equation 2 can be defined as the relationship of the shedding frequency to the flow velocity [6].

$$U_r = \frac{U}{f_{sh}\ D} \tag{2}$$

Instability at the boundary layer can lead to organized, unsteady, slow motion, or disorganized motion, regardless of whether the separating boundary layer is laminar or turbulent; periodic vortex shedding dominated accurses to the feature of the bluff body wake. A circular cylinder pipe is focused on bluff bodies, and flow about it is ubiquitous in both natural and industrial applications [6]. Rabiee et al. [7], studied square-section cylinders placed side by side. At low Reynolds numbers, they found that the control unit effectively reduces the vibration of the rear and front cylinders by up to 94% at R_e= 80 and 97% at R_e= 100. Gao et al. [8], studied an active flow control method at the R_e equals to 1.67 × 10^4 using jets integrated at a square cylinder's front and rear stagnation points to suppress unsteady wake flow. Particle image velocimetry technique was used. Ren et al. [9], used high-resolution CFD simulations in machine learning-based active flow control to suppress (VIV) of a circular cylinder at R_e= 100, using blowing/suction at fixed locations. Applying this control law suppresses 94.2% of the VIV capacitance and achieves 21.4% better overall performance than the best open-loop controllers. Zhu et al. [10], conducted a study based on numerical research to evaluate the efficiency of an active control method at a low Reynolds number using a pair of air jets placed on both shoulders of a circular cylinder. The vibration control becomes more effective as the momentum coefficient increases. A reduction of more than 60% in transverse capacity was achieved.

In many industrial applications, vibration control is an important topic of concern. Unwanted vibration may negatively impact the structure, sometimes resulting in disastrous results. Different techniques have been developed to control vibrations in a system. These approaches and strategies include actuators or sensors. Passive and active control systems are used to control the vibration of structures subjected to wind [11]. Active control techniques, which include energy input to a flow-structure system via actuators or other ways to bring about desired changes to the system, may be either closed-loop or open-loop [12]. For example, Joshi et al. [13], investigated the different flow control techniques and developments. Through this comparison, they were able to conclude that active flow control technology has clear advantages compared to passive control. Muddada et al. [14] proposed a simple active flow control strategy based on momentum injection at low Reynolds numbers. Two small control cylinders located at an angle of 120 degrees behind the main cylinder are actuators. They found that the complex vortex structures behind the main circular cylinder are controlled by using two small rotary control elements, and the closed loop effectively repressed the induced oscillations. Hasheminejad et al. [15], conducted a numerical study on a laminar crossflow condition for a wide range of reduced flow velocities of circular cylinders fitted with the actuator. Three different feedback control configurations are used: push-button actuation control and hybrid actuation control. The displacement response control performance of hybrid actuation control designs has been found to significantly outperform that of force-actuated or pressure-actuated systems. Malarczyk et al. [16], suggested an active vibration damping control system independent of piezoelectric actuators and using an accelerometer sensor for a long cantilever bite support system in a wind tunnel. A self-adaptive fuzzy ratio differentiation (PD) control model is proposed to realize automatic adjustment of control parameters for different test conditions. Bai et al. [17], studied the vibration of wind turbine towers in wind turbine towers by using an active damper named the Twin Rotor Damper (TRD), comparable to a passive adjust-it mass damper. The findings indicate that the TRD is effective in reducing vibrations on the wind turbine towers. Based on previous studies, many researchers have used control methods to obtain the best performance to reduce wind-induced vibration of cylindrical pipes by adjusting actuators in different applications. Therefore, the main contribution of this work was to reduce the vibration on the pipes to obtain optimal stability using a control device (CRBCP), which had not been used before in this application. The objectives of the study are to reduce wind-induced vibration by using electrical energy to enhance system efficiency and to develop a model using actuators. Finally, CRBCP and vibration control of cylindrical pipes are used to maintain stability within acceptable pavement.

2. VIV Experimental setup

In this study, a hollow circular cylinder pipe model was designed and manufactured under VIV, the influence of data collection, which is done by using the necessary tools such as the accelerometer, sensor of flow rate, signal condition, and data acquisition (DAQ). The data collection flow chart applied in the experiment shows the process shown in Figure 1 [18].

The wind tunnel is designed as an open-shaped wind tunnel for the entire airflow inside the test area. The wind tunnel has open circuit specifications, and the reason for choosing this type is due to the ease of manufacturing and implementation; an open wind tunnel is used to generate airflow with different velocities through the test section. Figure 2a shows the schematic diagram design of wind tunnel and Figure 2b shows the actual product of the low-speed wind tunnel. The wind tunnel device consists of three main sections. The test section, the contraction section, and the diffuser section. The contraction area ratio (a_c) is defined by the Equation 3 [19].

$$a_c = \frac{cross-sectional\ area\ at\ entry\ to\ contraction\ cone}{cross-sectional\ area\ at\ exit\ to\ contraction\ cone} = \frac{A_1}{A_2} \tag{3}$$

In aerodynamic research, a wind tunnel is used to investigate the effects of air passing through solid objects, the forces acting on them, and their interaction with the airflow [19].

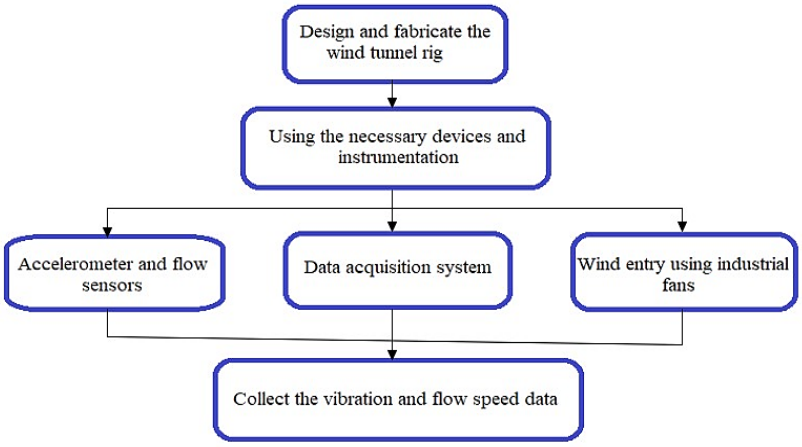

Figure 1: Experimental data collection flow chart

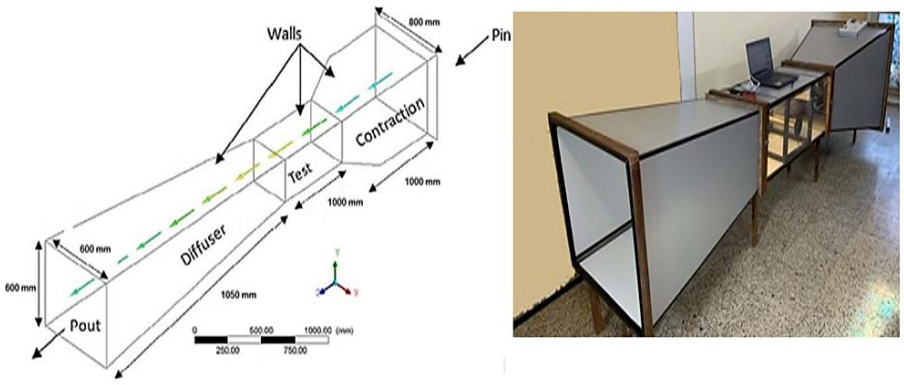

(a) **(b)**

Figure 2: The proposed diagram of wind tunnel (a) Wind tunnel design (b) Real wind tunnel

The wind tunnel was of the traditional open-direction non-return type with the test work section part closed. It was constructed and executed from pressed aluminum composite panels with a thickness of 4 mm. The dimensions of the wind tunnel were an overall length of 3.2 m, a width of 0.88 m, and an average height of 1.2 m at the level of the earth [19, 20]. The wind velocity inside the open wind tunnel of the test section was controlled by the use of four fixed industrial fans, each motor 120-watt, 2500 rpm, and a drive unit with a regulator speed control unit. The four propellers' size and motor speed range are designed to provide wind speeds from 1 m/s to 10 m/s through a wind tunnel over the test section. A smart wheel anemometer positioned 1.12 m upwind from the end of the wind tunnel was used to measure wind velocity [3].

A single hollow aluminum cylinder vibrating in the direction of wind flow connected to a spring mounted on a circular plate on either side of the cylinder pipe is designed and manufactured. The configuration of the segmented circular cylinder pipe model is included, as shown in Figure 3. A list of the parameters used in the experimental study is shown in Table 1.

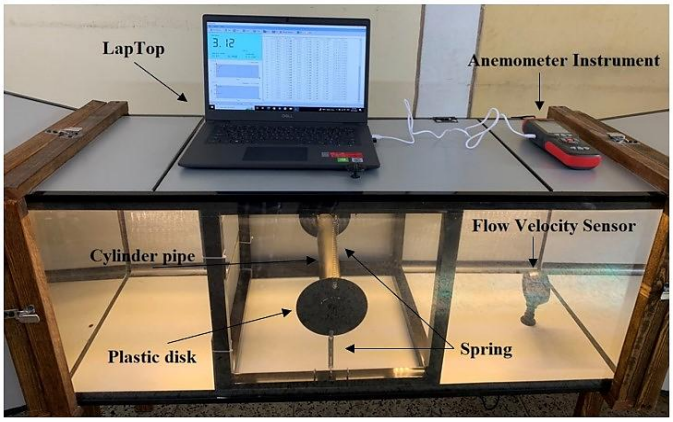

Figure 3: Circular cylinder pipe model

Table 1: Experimental details of the VIV test

Parameters	Symbols	Values	Units
Cylinder diameter	D	50	mm
Cylinder length	L	300	mm
Aspect Ratio	L/D	6	Dimensionless
Mass of cylinder	M	0.420	Kg
Mass ratio	m^*	582	Dimensionless
Stiffness of system	k	68.67	N/m
Reynolds number	Re	3333-33333	Dimensionless
Wind flow speed	U	1-10	m/s

The mass effect is determined by parameters called the mass ratio (m^*). This can be defined as the ratio of the oscillating structural mass of a cylinder in air (M_{osc}) to the mass of the displaced fluid impinging on the vortex-induced vibration (M_{air}).

$$m^* = \frac{M_{osc}}{M_{air}} \tag{4}$$

where

$$M_{air} = \frac{\pi}{4} \rho D^2 L \tag{5}$$

$$m^* = \frac{4M_{total}}{\pi \rho L D^2} \tag{6}$$

M_{total} is the total vibration system mass, ρ is the fluid density, D is the outer diameter of the cylinder, and L is the cylinder length. Free vibration studies are difficult to analyze because of the link between decreased velocity (shedding frequency normalized by natural frequency) and the ratio of amplitude (amplitude normalized by cylinder diameter). To ensure that circumvent this problem, forced vibration studies are used to investigate one element at a time. Forced vibration studies may give knowledge that free vibration testing cannot directly supply [21]. Numerous instruments and techniques have been used to simulate the (VIV) phenomenon, including the fans that are used to push the wind inside the tunnel at different speeds, data acquisition systems, and sensors integrated to collect the data for vibration to the computer [22, 23].

3. Control strategies

3.1 Technique of passive control

The passive control technique provides the experimental suppression of the hollow cylinder pipe model deflection by using a double control rod located in positions, which Control Rod Beside the main Cylinder Position (CRBCP). When the double control rods were fixed as shown in Figure 4, two different configurations of the control rod's location were used to apply a trial-and-error method of passive vibration control. The distance of 10 mm between the control rod's circumference and the main circular cylinder circumference was set to enable AVC with control rods with a diameter of 10 mm. It has been noted that there is some suppression at less than 8 mm. This is considered with different range distances, which was chosen to avoid cylinder pipe suppression, apply active control in the step, and demonstrate the true performance of the active control technique [23].

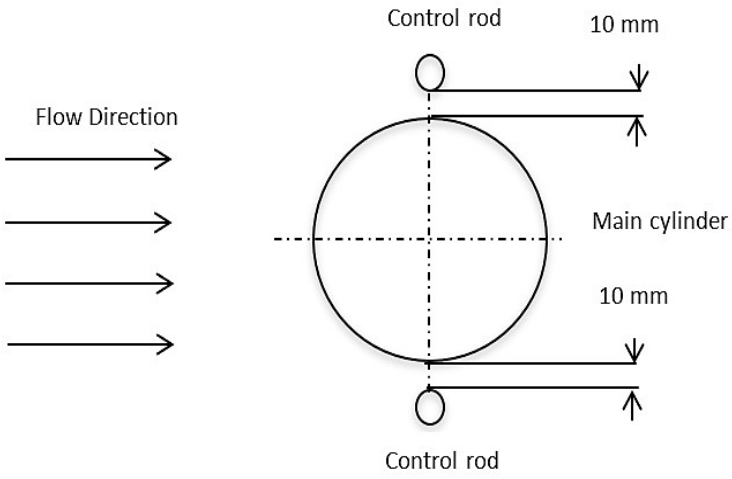

Figure 4: Diagram of control rods beside the main cylinder position (CRBCP)

The double-control rods were positioned in the hollow circular cylinder pipe about the incoming wind flow configuration of the main cylinder. A NI-USB 6009 device (DAQ) has been employed via the accelerometer GY-61 ADXL335 sensor to accomplish the passive control technology using the computer analog inputs port via DAQ, as illustrated in Figure 5. Using the required equipment, the same process has been used to record the amplitude vibration of the cylinder pipe [24].

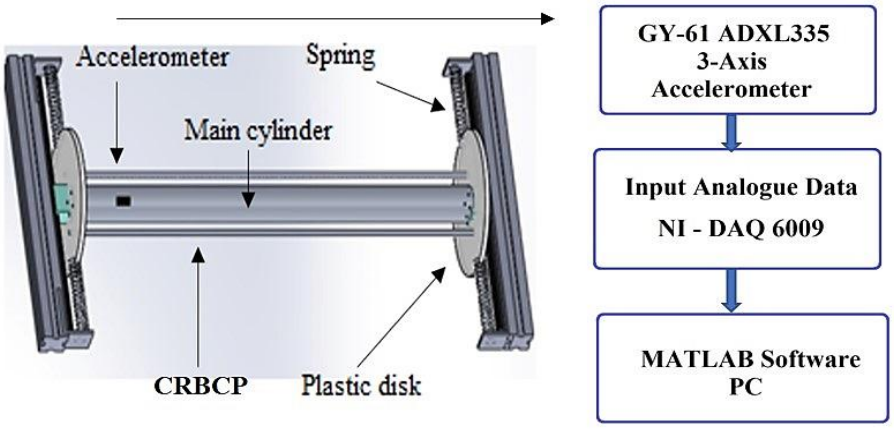

Figure 5: Schematic diagrams of output data collection

3.2 Active of open-loop vibration control

Vibration control with active open loop technique, which was not possible with passive control to suppress the unwanted vibration on the cylindrical pipe induced by (VIV) is covered in this section. The actuators for open-loop control are composed of two small 12V DC motors with speed (0 to 3000) rpm that drive double control rods, and an external power supply is situated atop the rods. The motors were configured so they could turn the rods in both CW and CCW directions. The workflow is illustrated by block diagrams in Figure 6 [25].

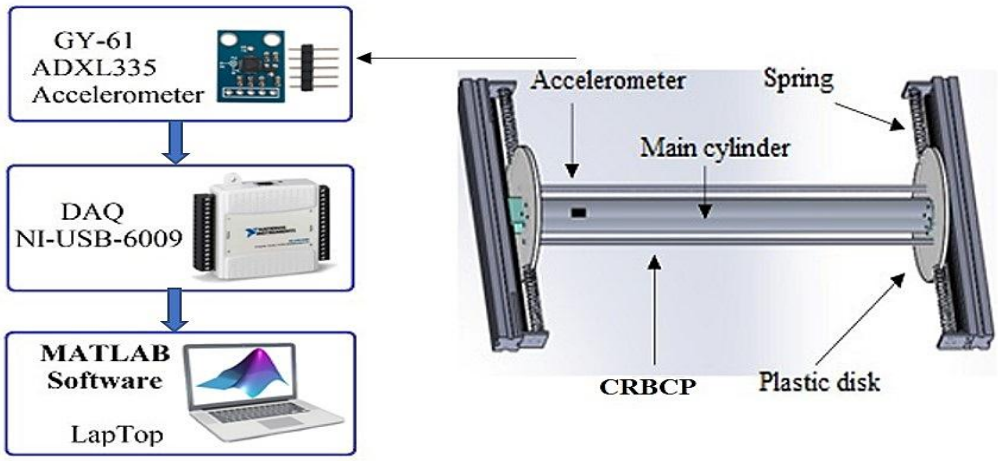

Figure 6: Data collection setup for control

Two location places were chosen for the rods. As shown in Figure 7, the DC motors received their voltage directly from an AC-DC power supply through driver L298N controlling DC motors. Furthermore, a MATLAB 21 software application was utilized to configure, receive, and transmit the signal from accelerometers to the DC motor through DAQ NI-6009. Almost all electronic devices need a DC supply for smooth operations, and they need to operate within certain power supply limits. A regulated linear power supply is used to ensure that the output remains constant even if the inputs change. The regulated linear DC power supply is also called a power supply. The double H driver module uses an L298N dual full-bridge driver, an integrated circuit. It is a high voltage, high current dual full-bridge driver designed to accept standard logic levels and drive inductive loads such as relay and DC motors, etc. The input data are provided, and the signal will used to input in ways to turn the device on or off independently of input signals [26]. Figure 8 shows the design and implementation aspects of the hollow cylinder vibration control system, which consists of DC motors and rods to control the vertical vibration of the cylinder pipe [26].

Figure 7: Output rotational speed generation process through L298N and power supply

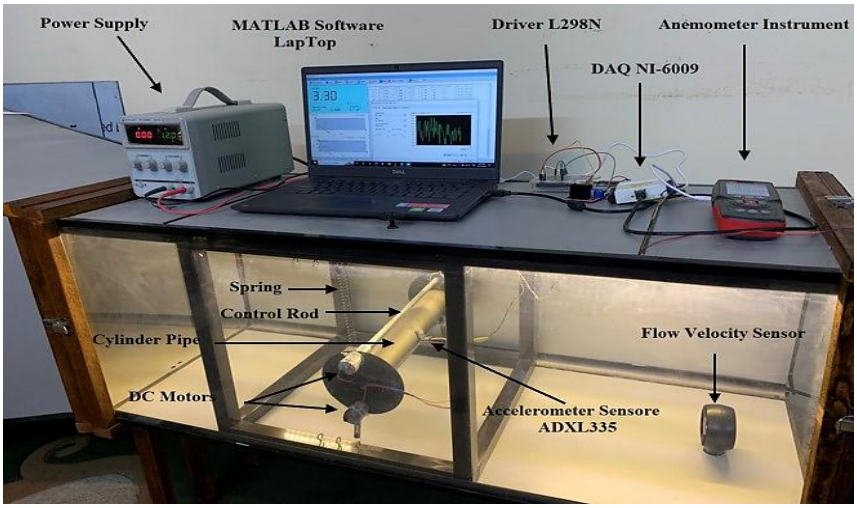

Figure 8: Main components for a control system in the side test section of a wind tunnel

4. Results and discussion

4.1 Experimental vibration and flow velocity results

Wind flow velocity is the determination of the value of wind speed at a certain rotation of the fans. This study uses the input parameter based on the wind speed and the rotation of the fan device, which have been shown clearly. This subsection provides the cylindrical pipe deflection caused by VIV and the wind flow velocity. Table 2 displays the data on wind flow velocity that were collected using software and an anemometer sensor.

Table 2: The parameter has been design based on wind flow velocity measurement

Test No.	Fan speed rotation (RPM)	Max flow velocity (m/s)	Min flow velocity (m/s)	Average flow velocity (m/s)	Reduced velocity
Test 1	140	1.12	O.95	1.01	9.85
Test 2	163	2.17	1.86	2.04	19.70
Test 3	472	3.16	2.91	3.00	29.56
Test 4	813	4.09	3.89	4.07	39.41
Test 5	909	5.12	4.91	5.02	49.26
Test 6	1130	6.41	5.79	6.03	59.11
Test 7	1440	7.19	6.85	7.04	68.96
Test 8	1787	8.52	7.97	8.19	78.82
Test 9	2036	9.19	8.85	9.08	88.67
Test 10	2349	10.32	9. 97	10.01	98.52

Propellers create wind flow, so the purpose of the measurement is to determine the value of the wind speed at a given rotation of the propellers. Values ranging from 140 to 2349 rpm were chosen for the propeller speed to study the effect of the deviation of the circular cylinder pipe model resulting from wind flow speeds of 1 to 10 m/s to determine the maximum deviation. The values were chosen inside the wind tunnel. Figure 9 shows the wind flow at different speeds from (a) 1 m/s to (j) 10 m/s.

Figure 9: Air flow velocity measured by varying the rotation of the fans (a) air flow at 1 m/s (b) air flow at 2 m/s (c) air flow at 3 m/s (d) air flow at 4 m/s (e) air flow at 5 m/s (f) air flow at 6 m/s (g) air flow at 7 m/s (h) air flow at 8 m/s (i) air flow at m/s and (j) air flow at 10 m/s

This section presents the time and frequency response to the vibration of a cylindrical pipe at different wind speeds from 1 to 10 m/s. The natural frequency of the free vibratory system structure can be analyzed and calculated using a simple mathematical, analytical formula, as shown in the attached equation $F_n=(1/2\pi)\sqrt{(K_{Total}/M_{Total})}$. The result of the analysis for the natural frequency was 2.048 Hz. The vibration frequency at the corresponding system responds to the maximum amplitude of vibration according to the speed of 10 m/s, shown in Figure 10a time response and Figure 10b frequency response, when the

amplitude values are obtained experimentally. The maximum amplitude of vibration of the cylindrical pipe was found at maximum speed compared to other wind speeds [25].

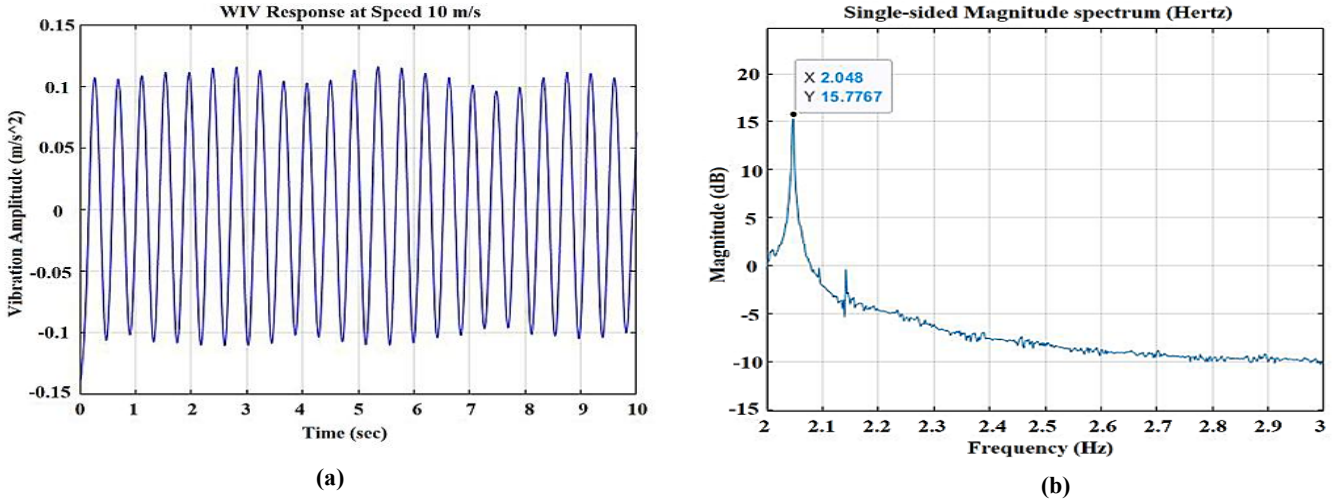

Figure 10: The response of wind flow velocity at 10 m/s (a) Time response (b) Frequency response

After determining the working range of the wind speed that affects the vibration of the circular cylindrical pipe at 10 m/s, according to the length L of the hollow cylinder pipe (300 mm) and diameter (50 mm). The reason for the aspect ratio of the cylinder (L/D = 6), flow around the cylinder pipe. It can have a significant impact on the vortex dynamics, and the interdependence of fluid forces induced on the body and thus vibrations is determined and calculating the dimensionless values of reduced velocity, the Reynolds number dimensionless values.

4.2 Passive techniques

The study has been taken into two cases. In the first case, the passive control techniques were utilized to verify dual control rods when inserted next to the main cylinder pipe. At the upper and lower of it, it was observed that the effect of wind vortices on the cylindrical pipe, which caused vibration, led to the breaking of these vortices formed behind the cylindrical tube, which led to the suppression of vibration. Figure 11a shows the frequency response and Figure 11b shown the time response of hollow cylinder deflection using dual control rods next to the cylinder pipe and at the upper and lower of the hollow cylinder pipe. It was discovered that control rods were introduced into the system. The amplitude deflection of the cylinder pipe was slightly reduced compared to the response of the pipe without adding controls rods. The amplitude value for the cylinder pipe without control rods positioned beside the cylinder pipe recording, the max deflection value 0.125 when the decrease velocity (Ur) was 98.52.

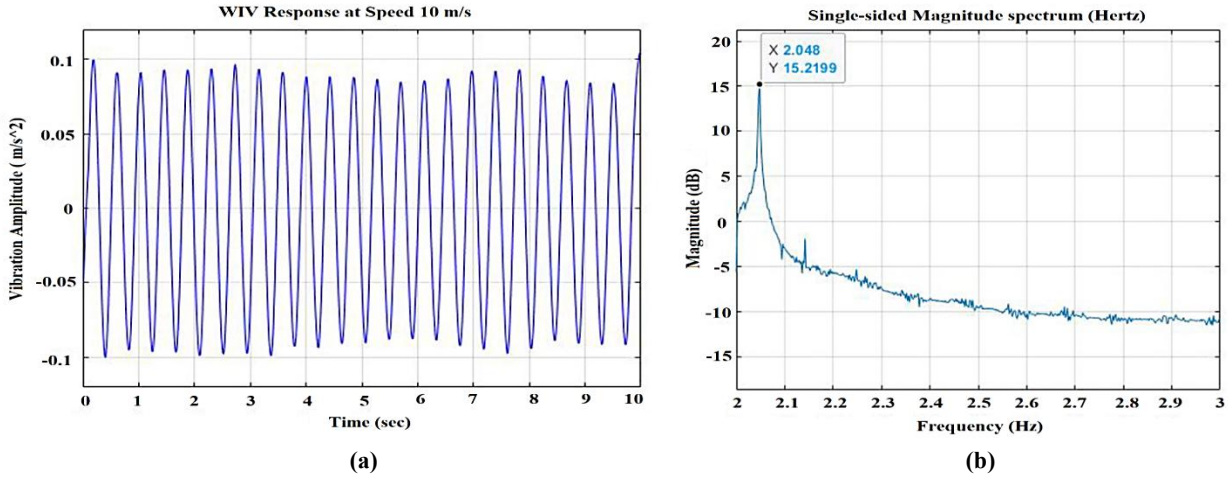

Figure 11: The response with adding a double DC motor and rods at wind flow velocity at 10 m/s (a) Time response (b) Frequency response

For the second case, the maximum cylinder pipe deflection with reduced velocity (Ur) at 98.52 resulted in an amplitude of 0.099, which had a control rod at the upper and lower of the master cylinder pipe. It was 20.8% less than the value recorded in the case study when there were no control rods. The weight supplied to the systems reduced the first mode amplitude of frequency values when compared to the systems without actuators. The result showed that the frequency value of the maximum cylinder

pipe deflections and reduced velocity of 98.52 should equal 2.048 Hz for CRBCP. The low-frequency values were caused by the inverse connection between frequency and mass, the added mass of the control rods, and other accessories.

4.3 OLAVC

4.3.1 Actuator direction at control rods position result

An electromechanical actuator was used on the circular cylinder pipe at the CRBCP to reduce vibration. The actuators were located at the upper and lower of the cylinder and at one where the rods were attached to the actuators through a coupling, as shown in Figure 12.

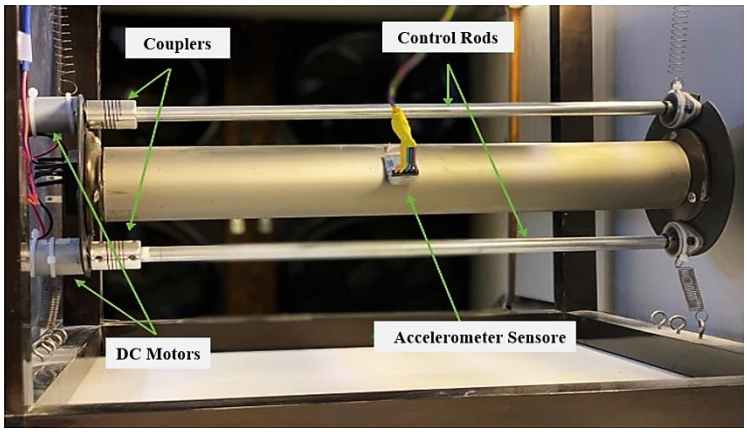

Figure 12: Cylinder pipe with control rods as a DC motors actuator

Both CW and CCW rotary motor directions are also considered. Initially, the CRBCP position was evaluated in both CW or CCW at the same directions for all motors with an average flow rate of 5 m/ss and a reduced velocity of 49.26, which resulted in maximum deflection of the cylinder pipe model. The actuator speed is used at 84% of the overall motor speed and approximately equal to 10 V as a technique of active open loop control; power was directly applied to the dual motors from an AC-DC power source at 10 V to drive the dual control rods. This procedure and measurement were also done using the DAQ NI-USB 6009 controller drive and computer system. Figure 13a shows the time response and Figure 13b shows the frequency response result of the cylinder pipe model under VIV, and the amount of expansion has decreased slightly, where both the upper and lower motors positions are oriented in the same direction, either CW or CCW, with the same speed, and the same control rod position.

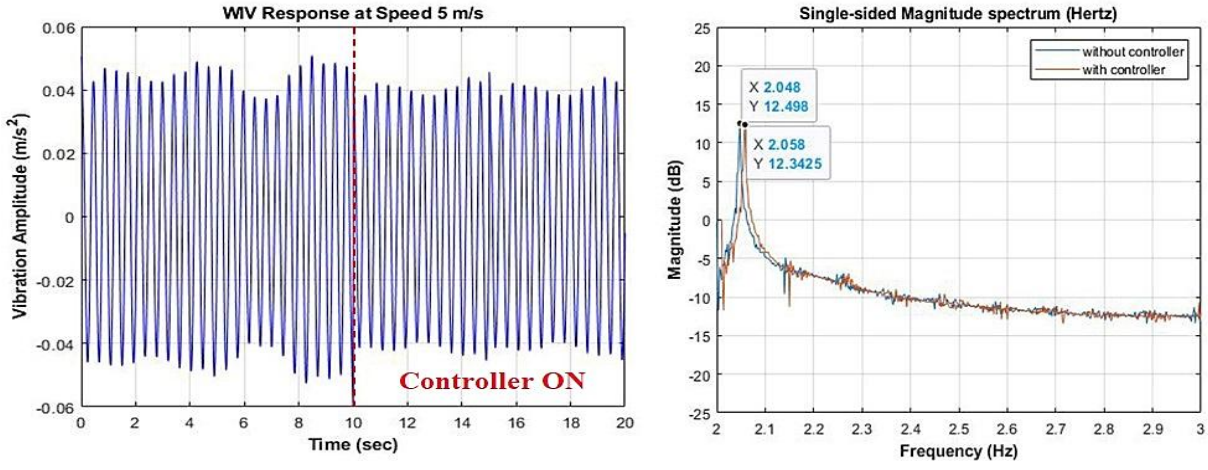

(a) **(b)**

Figure 13: The response at velocity 5m/s in the same direction CW or CCW for CRBCP (a) Time response (b) Frequency response

The magnitude of frequency value for the cylinder pipe deflections with CRBCP by using dual control rods in either a CCW or CW orientation to apply open loop active control, the magnitude frequency values were 12.498dB and 2.048Hz respectively, after applying passive control of 12.3425 dB and 2.058 Hz. With an attenuation level of 0.1528 dB, these technologies reduced vibration by as much as 13.639%. The results presented in Figure 14a (time response) and Figure 14b (frequency response) show the time and frequency responses of the cylinder pipe models subjected to vortex-induced vibrations (VIV) in the direction of actuator rotation. In this case, the upper actuator rotates counterclockwise (CCW), while the lower actuator rotates clockwise

(CW) at the same speed and with the same control rod position. It was observed that the expansion decreased more significantly than in the previous case.

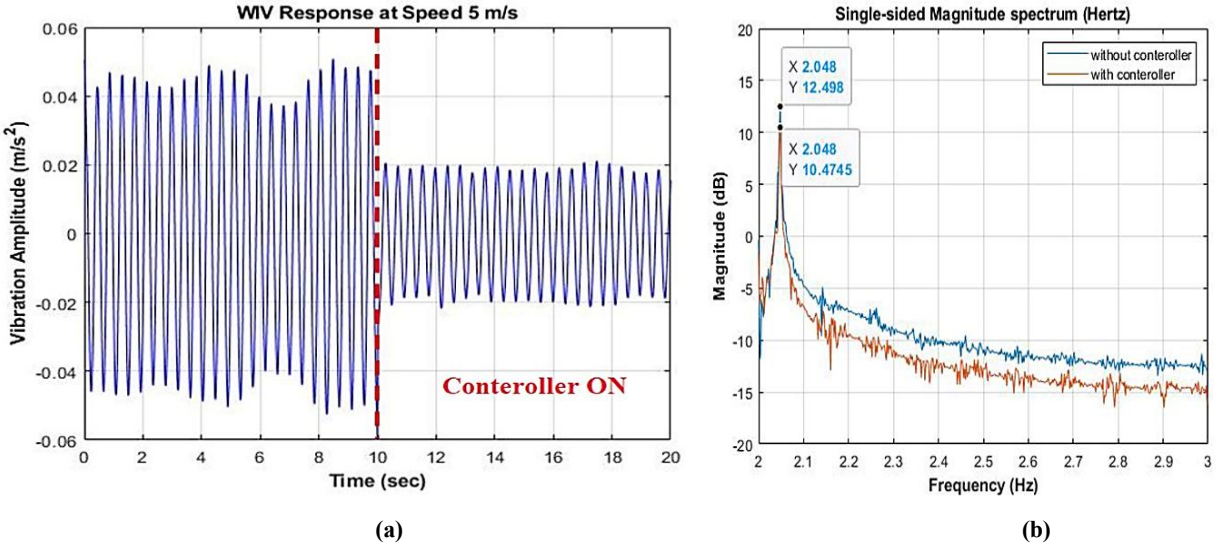

Figure 14: The response at wind speed of 5 m/s in the CW direction of the lower actuator and CCW of the upper actuator for CRBCP (a) Time response (b) Frequency response

The time and frequency response resulted when the control rods operated successfully in the CRBCP under VIV and when driven by dual motors with the direction of rotation CCW for the upper motor position and the direction of rotation CW for the lower motor position in reducing unwanted vibration compared to the direction of rotation CW or CCW for both motors at the same time.

The magnitude of frequency value for the cylinder pipe deflections with CRBCP by using double control rods in a CW or CCW direction to apply open loop active control, the magnitude frequency values were 12.3425 dB and 2.058 Hz, respectively, after applying passive control of 12.498 dB and 2.048 Hz, with an attenuation level of 0.1555 dB, passive technologies reduced vibration by as much as 8.39%. However, the values of the magnitude and frequency of the cylinder pipe deflection using CRBCP as a passive control were 12.498 dB and 2.048 Hz. In comparison, the magnitude and frequency values after applying active open-loop control via dual control rods in the CW and CCW directions were 10.474 dB and 2.048 Hz. Passive technology decreased vibration by as much as 61.82% with amplitude levels of signal. An identical process was carried out to study the effect of kinematic directions on the deflection of the cylinder pipe of CRBCP. Figure 12 shows the frequency and time response results of the cylinder pipe model resulting from WIV in the CW direction results for both rods or CCW for both rods. Figure 13 displays the time and frequency response results of the cylindrical pipe model generated by WIV when the control rods are rotated in the direction CCW of the upper rod position and CW of the lower rod position. As a result, the direction when the control-rods motor is rotated in the directions of CCW of the upper rod position and the CW motor of the lower rod position was successful in lowering the generation of vortices behind the cylinder pipe due to the direction of the control-rods, which reversed the wind flow directions resulting in slighting turbulence after the control-rods and preventing the vortices from taking enough time to produce it.

4.3.2 Vibration analysis of OLAVC during various disturbances

Different perturbations were used to test the performance of the cylinder pipe model. OLAVC technology uses an electromechanical actuator on which two rods are mounted, one rod at the upper and the other rod at the lower of the master cylinder position. The OLAVC approach was based on the use of an electromechanical actuator incorporating a CRBCP and dual DC motors rotating CCW for the upper motor and CW for the lower motor. The upper and lower motors are supplied with constant voltage from the power supply of 6, 8, 10, and 12 volts, which is equal to 50, 66, 83, and 100% of the motor power efficiency in all different types of disruption. Real turbulence was carried out using four electric fans whose speed was controlled using a variable resistance voltage regulator with wind speed change values ranging from 314 to 2500 rpm, and the speed value of the propeller of 2349 rpm caused the maximum height of the cylindrical pipe model deflection. The performance of the hollow cylindrical pipe under actuator excitation in the CRBCP system, at a disturbance speed of 2349 rpm, is illustrated in Figure 15. Specifically, Figure 15a shows the response at an actuator voltage of 6 V, Figure 15b at 8 V, Figure 15c at 10 V, and Figure 15d at 12 V. Both control rods' positional actuators (CRBCP) were rotated CCW for the upper actuator and CW for the lower actuator, suppressing undesired vibration with various actuator voltages. From the observed results, vibration suppression at 12V was achieved for both control rods' positions with CRBCP. In contrast, research [22] shows that the greatest vibration reduction occurred when the control rods were rotated in the same direction.

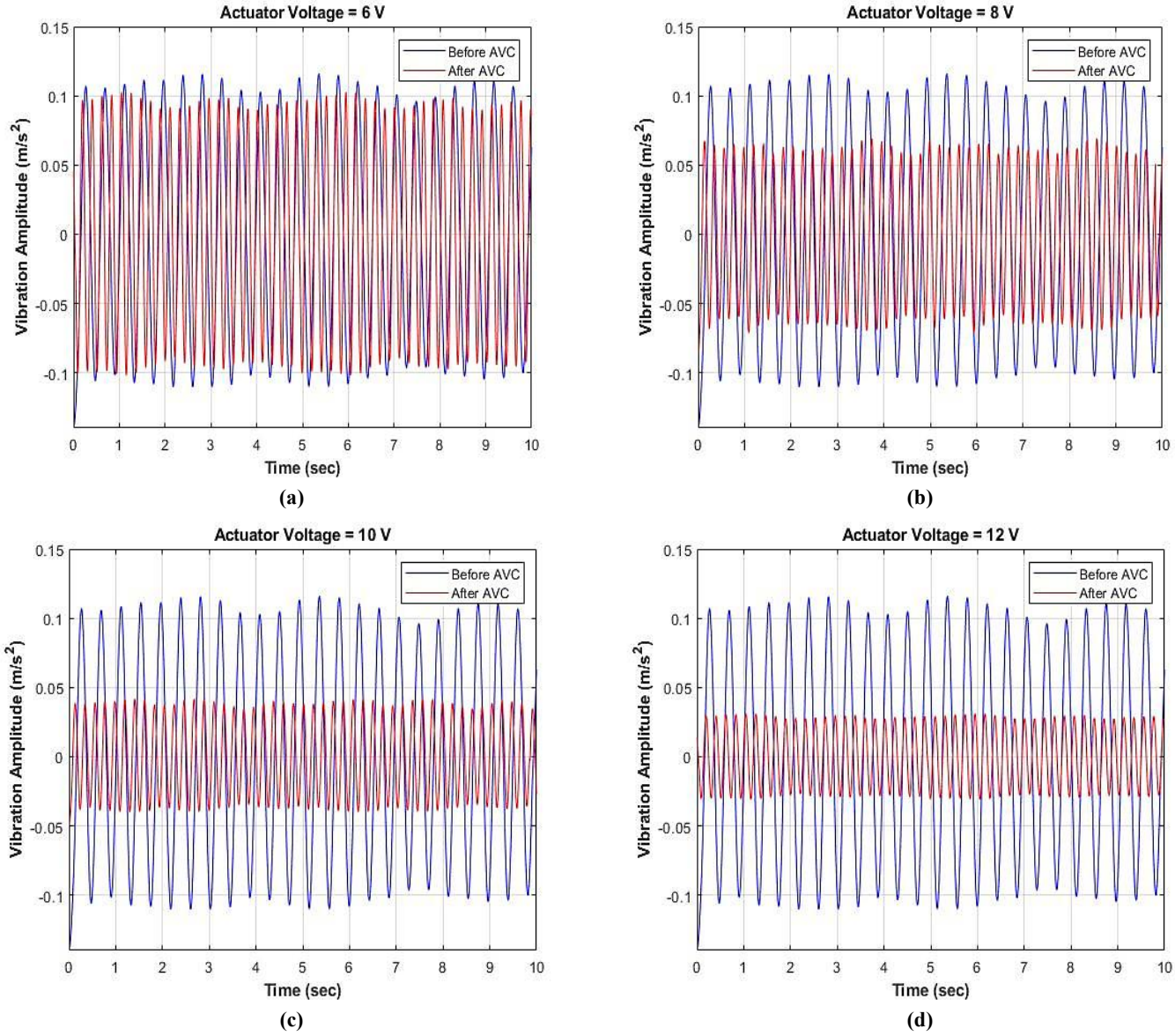

Figure 15: The time response in CCW for upper rod and CW for lower rod directions in CRBCP (a) Actuator voltage of 6V (b) Actuator voltage of 8V (c) Actuator voltage of 10V and (d) Actuator voltage of 12V

It is generally observed from these results that the best results it was achieved that the best vibration suppression was achieved suppression of vibration of the cylindrical tube exposed to varying wind speeds at 12 volts was achieved for both actuators when the upper actuator rotated CCW and the lower actuator rotated CW. The reason behind this is that the CRBCP is close to the eddies on both sides. As actuator voltages increased, the vibration amplitude gradually decreased, with the largest decrease seen at 10 and 12 V for both actuators.

4.3.3 Frequency analysis of OLAVC during various disturbances

The performance of OLAVC was best demonstrated through the display of frequency plots under difficult wind flow velocity perturbations. Figure 16 shows the result of the frequency response of the hollow cylindrical pipe performance in CW and CCW for CRBCP. We observe that the amount of amplitude in the signal decreases when the amount of voltage supplied to the control system increases by 6, 8, 10, and 12 V compared to the absence of the control system at the same flow speed.

Tables 3 and 4 show the reduction levels at different wind disturbances with and without the use of OLAVC technology at all disturbance frequencies. Table 5 shows the observance result of the magnitude reduction level in the CCW of upper rod direction and CW of lower rod directions for CRBCP at disturbance fans 163 - 909 rpm.

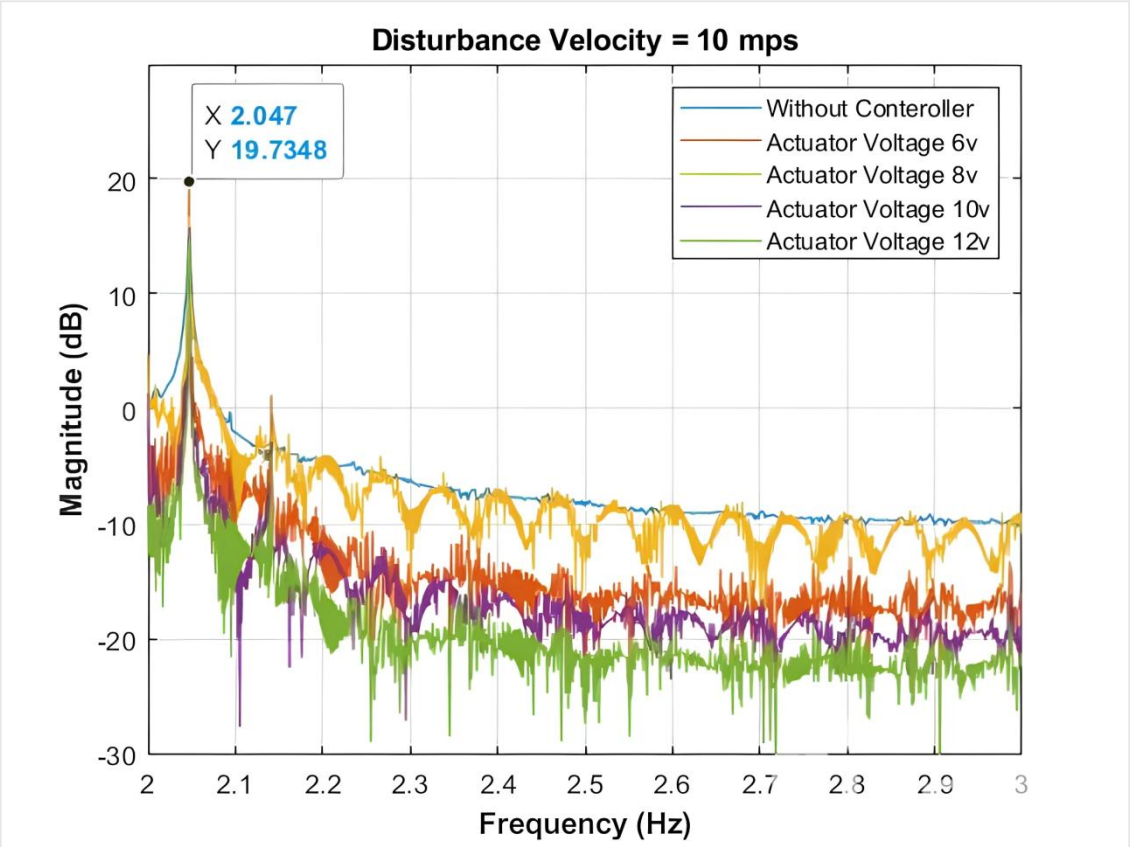

Figure 16: Frequency response results in CCW for upper rod and CW for lower rod directions in CRBCP

Table 3: Magnitude reduction level in CW and CCW direction rotation rods in CRBCP at disturbance 163 - 909 rpm

Actuator Voltage (V)	Magnitude Reduction level at 163 rpm (dB)	Magnitude Reduction level at 472 rpm (dB)	Magnitude Reduction level at 813 rpm (dB)	Magnitude Reduction level at 909 rpm (dB)
6	1.718	1.655	2.904	2.290
8	2.793	4.769	4.733	5.418
10	4.456	8.812	8.228	8.048
12	8.426	10.360	11.177	9.686

Table 4: Magnitude reduction level in CW and CCW direction rotation rods in CRBCP at disturbance 1130 – 2349 rpm

Actuator Voltage (V)	Magnitude Reduction level at 1130 rpm (dB)	Magnitude Reduction level at 1440 rpm (dB)	Magnitude Reduction level at 1787 rpm (dB)	Magnitude Reduction level at 2036 rpm (dB)	Magnitude Reduction level at 2349 rpm (dB)
6	2.428	2.416	3.692	3.977	2.905
8	5.019	4.882	8.371	5.851	9.808
10	9.453	11.998	10.778	10.679	11.857
12	11.874	13.539	13.748	14.507	12.845

The study found that the proposed strategy reduced unwanted vibrations. The best performance were obtained utilizing a motor voltage of 12 volts. When the flow is disturbed at 2036 rpm, record the max deflection of the cylinder pipe without using the control technique or applying a passive control model. The magnitude level was decreased by the active open loop control technique to 3.977, 5.851, 10,679, and 14,507 dB using 6, 8, 10, and 12 volt actuator voltages, respectively. It is concluded that as the actuator speed increases, the system's vibration magnitude reduction levels also increase, and its peak decreases. This was due to the effect of the control rod's rotating speed, which affected the system's vibrating frequency.

Finally, Table 5 presents the magnitude suppression percentages corresponding to motor voltages and disturbance frequencies ranging from 163 to 2349 rpm. It can be concluded that as actuator speeds increase, the system vibration magnitude reduction levels also increase, and their peak also decreases. This is due to the rotation speed of the control rods, which affects the system's vibration frequency. Ultimately, the conclusion can be reached that at dual actuator speed, the attenuation level increases with turbulence increasing considerably at both positions.

Table 5: Vibration suppression percentage for CRBCP in a CW and CCW direction

Disturbance speed (rpm)	Vibration suppression percentage at motor voltage (%)			
	6 V	8 V	10 V	12 V
163	14.67	23.85	38.05	71.96
472	12.18	35.11	64.88	76.28
813	19.44	31.69	55.09	74.83
909	15.73	37.23	55.31	66.57
1130	14.45	29.87	56.26	70.67
1440	13.62	27.53	67.67	76.36
1787	20.24	45.89	59.08	75.36
2036	21.67	31.88	58.19	79.05
2349	14.72	49.70	60.08	65.09

5. Conclusion

The models of passive and active open loop controls were demonstrated using dual control rods operated by DC motors located beside the master cylinder pipe and mounted at the upper and lower of the hollow cylinder pipe model. The experimental rig was designed and manufactured based on previous studies. In addition to collecting data by DAQ NI-6009 data acquisition device, the following was achieved:

1) Passive control technology proves ineffective in mitigating the vibrations of a hollow circular cylinder pipe when there is a 10 mm gap between the cylinder pipe and the rods. Only minimal suppression is achieved when the distance is reduced to less than 6 mm. Due to this limitation, AVC technology was developed to suppress vibration effectively.
2) Two motors rotate the control rods in the upper and lower positions of the hollow cylindrical pipe models to prevent vibration of the pipe. The best results were obtained when the upper rod was rotated in the CCW direction while the lower rod was rotated in the CW direction.
3) The use of an electromechanical actuator effectively eliminated the vortex formation behind the cylinder, resulting in a significant reduction of vibration.
4) The use of an electromechanical actuator is composed of dual control rods driven by two motors in (upper and lower) positions of the master cylinder pipe and connected by couplers to the direction of the DC motor were tested to determine the optimal directions to be used in open-loop active control technology. The CCW directions of the upper rod and the CW direction of the lower rod suppress the cylinder pipe vibration, greater than the CW direction of both control-rod positions.
5) The motors are provided with different voltages to rotate the control rod for both positions in the CCW and CW movement directions. All DC motor voltages were capable of reducing vibration at 12 V for both control rod locations of the CRPCP.
6) Passive and active control strategies were used to rotate the control rods. The control actuators were supplied with voltages of 6, 8, 10, and 12 volts to increase the speed of the control actuators. It was observed that at 12 volts, the best results were for the speed of rotation of the control actuators to suppress the vibration of the cylindrical pipe.

Author contributions

Conceptualization, **F. Jasim**, **M. Mohammed** and **H. Kadhom**; data curation, **F. Jasim**, **M. Mohammed** and **H. Kadhom**.; formal analysis, **F. Jasim**, **M. Mohammed** and **H. Kadhom**.; investigation, **F. Jasim**, **M. Mohammed** and **H. Kadhom**.; methodology, **F. Jasim**, **M. Mohammed** and **H. Kadhom**.; project administration, **F. Jasim**, **M. Mohammed** and **H. Kadhom**, resources, **F. Jasim**; supervision, **M. Mohammed** and **H. Kadhom**.; validation, **F. Jasim**, **M. Mohammed** and **H. Kadhom**.; visualization, **M. Mohammed** and **H. Kadhom**; writing—original draft preparation, **F. Jasim**.; writing—review and editing, **F. Jasim**, **M. Mohammed** and **H. Kadhom**. All authors have read and agreed to the published version of the manuscript

Funding

This research received no specific grant from any funding agency in the public, commercial, or not-for-profit sectors.

Data availability statement

The data that support the findings of this study are available on request from the corresponding author.

Conflicts of interest

The authors declare that there is no conflict of interest.

References

[1] S. Muddada, B. S. V. Patnaik., Active flow control of vortex-induced vibrations of a circular cylinder subjected to non-harmonic forcing, Ocean Eng., 142 (2017) 62-77. https://doi.org/10.1016/j.oceaneng.2017.06.036

[2] Yang, Y. Experimental investigations of vortex induced vibration of a flat plate in pitch oscillation. Ph.D. Thesis, Texas A & M University, 2012. https://hdl.handle.net/1969.1/ETD-TAMU-2010-12-8984

[3] Yang, Y. Experimental investigations of vortex-induced vibration of a flat plat in pitch oscillation. M.Sc. Thesis, Texas A&M University, 2010.

[4] X. Fan, Z. Wang, X. Chen, Y. Wang, W. Tan., Experimental investigation on flow-induced vibration of flexible multi cylinders in atmospheric boundary layer, Int. J. Mech. Sci., 183 (2020) 105815. https://doi.org/10.1016/j.ijmecsci.2020.105815

[5] Wen-Li Chen, Y. Haung, Ch. Chen, Review of active control of circular cylinder flow, Ocean Eng, 258 (2022) 111840. https://doi.org/10.1016/j.oceaneng.2022.111840

[6] C. Block, J. Engelhardt, F. Henkel, Active Control of Vibrations in Piping Systems, 20th International Conference on Structural Mechanics in Reactor Technology, SMiRT 20-Division 6, (2009) 1658-1666.

[7] A. H. Rabiee, F. Rafieian, A. Mosavi, Active vibration control of tandem square cylinders for three different phenomena Vortex induced vibration, galloping, and wake-induced vibration, Alexandria Eng. J., 61 (2022) 12019–12037. https://doi.org/10.1016/j.aej.2022.05.048

[8] D. Gao, H. Meng, Y. Huang, G. Chen, Wen-Li Chen, Active flow control of the dynamic wake behind a square cylinder using combined jets at the front and rear stagnation points, Phys. Fluids, 33 (2021) 047101. https://doi.org/10.1063/5.0043191

[9] F. Ren, Ch. Wang, H. Tang, Active control of vortex-induced vibration of a circular cylinder using machine learning, Phys. Fluids, 31 (2019) 093601. https://doi.org/10.1063/1.5115258

[10] H. Zhu, T. Tang, H. Zhao, Y. Gao, Control of vortex-induced vibration of a circular cylinder using a pair of air jets at low Reynolds number, Phys. Fluids, 31 (2019) 043603. https://doi.org/10.1063/1.5092851

[11] M. Farsi, M. J. Shariatzadeh, M. A. Bijarchi, E. P. Masouleh, M. B. Shafii, Low-speed wind energy harvesting from a vibrating cylinder and an obstacle cylinder by flow-induced vibration effect, Int. J. Environ. Sci. Technol., 19 (2021) 1261-1272. https://doi.org/10.1007/s13762-021-03241-1

[12] L. Cheng, Y. Zhou, M. M. Zhang, Controlled vortex-induced vibration on a fix-supported flexible cylinder in cross-flow, J. Sound Vib., 292 (2006) 279-299. https://doi.org/10.1016/j.jsv.2005.07.044

[13] S N. Joshi, Y. S. Gujarathi, A review on active and passive flow control techniques, Int. J. Recent Technol. Mech. Elec. Eng., 3 (2016) 1-6.

[14] S. Muddada, B. S. V. Patnaik, Active flow control of vortex induced vibrations of a circular cylinder subjected to non-harmonic forcing, Ocean Eng. 142 (2011) 62-77. https://doi.org/10.1016/j.oceaneng.2017.06.036

[15] S. M. Hasheminejad, Y. Masoumi, Hybrid active flow induced vibration control of a circular cylinder equipped with a wake-mounted smart piezoelectric bimorph splitter plate, J. Fluids Struct., 110 (2022) 103531. https://doi.org/10.1016/j.jfluidstructs.2022.103531

[16] M. Malarczyk, M. Zychlewicz, R. Stanislawski, Speed Control Based on State Vector Applied for Electrical Drive with Elastic Connection, Automation J., 3 (2022) 337-363. https://doi.org/10.3390/automation3030018

[17] H. Bai, Y. Aoues, J. M. Cherfils, D. Lemosse, Design of an Active Damping System for Vibration Control of Wind Turbine Towers, Infrastruct. J, 6 (2021) 1-24. https://doi.org/10.3390/infrastructures6110162

[18] M. J. Mohammed, I. Z. Mat Darus, N. M. Ridzuan, A. A. AL-Khafaji, Open Loop Active Control Technique on Segmented Marine Riser Vibration Using Electromechanical Actuator, Iran J. Sci. Technol. Trans. Mech. Eng., 43 (2018) 799-813. https://doi.org/10.1007/s40997-018-0229-y

[19] N. Verma, B. D. Baloni, Numerical and experimental investigation of flow in an open-type subsonic wind tunnel, SN A. Sci. J., 1 (2019) 1384. https://doi.org/10.1007/s42452-019-1422-3

[20] S. Yang, Yi. Experimental investigations of vortex induced vibration of a flat plate in pitch oscillation. Ph.D. Thesis, Texas A & M University, 2012. https://oaktrust.library.tamu.edu/items/da17311c-5fd2-4afe-bfc6-5f65d008f704.

[21] X. Fan, Z. Wang, Y. Wang, W. Tan, The effect of vortices structures on the flow-induced vibration of three flexible tandem cylinders, Int. J. Mech. Sci., 192 (2020) 106132. https://doi.org/10.1016/j.ijmecsci.2020.106132

[22] M. J. Mohammed, I. Z. Darus, System Identification of Pipe Cylinder Behavior Caused by Vortex Induced Vibration, Proceedings of the 14th International Conference on Robotics, Control and Manufacturing Technology (ROCOM'14), Kuala Lumpur, Malaysia at: Malaysia, 2014,186-193.

[23] B. O. Omijeh, N. Onyekachukwu, P. O. Nwachukwu, Comparative Analysis of Transformer and Transformer Less-Based Variable DC Power Supply, Int. J. Mod. Eng. Res., 3 (2013) 551-563.

[24] Mohammed, M. J. Active vibration control of vortex-induced vibration on segmented cylindrical marine riser model. Ph.D. Thesis, Faculty of Mechanical Engineering, Universiti Teknologi Malaysia, 2016.

[25] H. M. Nikoo, K. Bi, H. Hao, Passive Vibration Control of Pipe-in-pipe (PIP) Systems Subjected to Vortex Induced Vibration (VIV), Proceedings of the Twenty-seventh (2017) International Ocean and Polar Engineering Conference, San Francisco, California, USA, 2017,1271-1276.

[26] T. Biedermann, F. Kameier, R. Heinze, On the optimization of a cylinder/plate configuration with the aim to improve the energy harvesting of vortex-induced vibrations, J. Energy Challenges and Mechanic, 2 (2015) 68-74.